2014 IEEE International Conference on Robotics & Automation (ICRA)
Hong Kong Convention and Exhibition Center
May 31 - June 7, 2014. Hong Kong, China

Collaborative Bathymetry-based Localization of a Team of Autonomous Underwater Vehicles

Tan Yew Teck[1], Mandar Chitre[2] and Franz S. Hover[3]

***Abstract*— Without access to GPS and high-quality visual landmarks, many autonomous underwater vehicles (AUV) face a fundamental navigation vs. cost tradeoff: advanced navigation systems that might include an INS, Doppler velocity, or long-baseline acoustics are expensive. Supporting low-cost operations, this work focuses on collaborative positioning for a team of AUV's, given a bathymetric terrain map, and only an altimeter and acoustic modem on each vehicle. The joint localization is performed via decentralized particle filtering, where we extend the usual measurement model to allow received information to modulate the importance function. We investigate the impact on performance of sensor noise, communication interval and number of vehicles. Results are shown for bathymetry maps near St. John's Island, Singapore, and for the Charles River Basin, Boston. In the second case, we ran our algorithm with physical measurements from actual vehicles executing trajectories.**

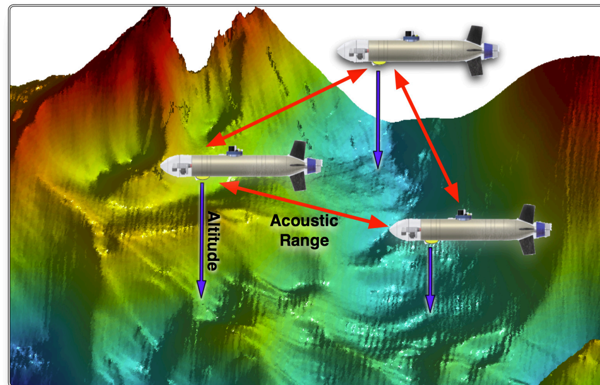

Fig. 1. Multi-AUV collaborative localization using altimeter measurements and inter-vehicle acoustic communications.

I. INTRODUCTION

Modern AUV's often carry proprioceptive navigation sensors such as an Inertial Navigation System (INS) and/or a Doppler Velocity Log (DVL). Although dead-reckoning from these sensors provides short-term positioning, accuracy will degrade over time. Surfacing periodically to get a GPS absolute fix may be an option for some missions, but surfacing can jeopardize the vehicles' safety when they are operating near busy shipping channels, or in rough seas. Surfacing from significant depth also consumes time and energy. Alternatively, navigation methods that involve deploying acoustic beacons are sometimes used. Among these are Long Baseline (LBL) [1], Ultra-Short Baseline (USBL) [2] and GPS Intelligent Buoy (GIB) [3] arrangements, which provide a georeference to correct an AUV's positioning errors. These methods not only require considerable operational effort, but they also are limited by their operating range, and are costly.

Current needs for lower-cost operation and for multi-vehicle missions have motivated interest in non-conventional navigation systems. As one approach, such systems may exploit seabed features. Bathymetry-based localization and navigation, also known as Terrain Relative Navigation (TRN) [4], Terrain-aided Navigation (TAN) [5], and Bathymetric-aided Navigation (BAN) [6] has gained the attention of researchers for its ability to keep positioning errors bounded. Given a bathymetric map, the idea of bathymetry-based localization is essentially to match a set of water depth measurements with the map, in order to estimate the vehicle's position. The performance of this localization technique obviously depends heavily on the variability of bathymetry in the area of operation. Bathymetry-based localization is possible for a single vehicle, but a multi-vehicle mission with communications and ranging capability can extend the possibilities considerably. Fitted with acoustic modems, AUVs today can exchange data packets, and exploit the travel time as a range measurement, e.g., [7]. The range measurements provide geometric constraints, and the data exchange enables a distributed localization process.

In this paper, we address the above considerations through a multi-vehicle underwater collaborative localization algorithm. The scenario is shown in Fig. 1.

[1]Tan Yew Teck is with Department of Electrical and Computer Engineering, National University of Singapore, Singapore. william@arl.nus.edu.sg

[2]Mandar Chitre is with Department of Electrical and Computer Engineering, National University of Singapore, Singapore. mandar@arl.nus.edu.sg

[3]Franz S. Hover with the Department of Mechanical Engineering, Massachusetts Institute of Technology, USA. hover@mit.edu

II. RELATED WORK AND PROBLEM FORMULATION

A. Background

Bathymetry-based localization generally employs sequential Bayesian filtering to estimate the probability of a vehicle being at a particular location in the map, using process and measurement models [4], [5], [6]. Since there is no closed-form solution for the *posterior* probability density, due to the highly non-linear bathymetric measurement model, we have pursued sequential Monte Carlo filtering methods [8]. One popular implementation is the Marginalized Particle Filter [9], [10], known for its computational efficiency in approximating the density function. In several marine applications, the data for the vehicle's measurement model are provided by on-board multi-beam echo sounders [4], [11]. This enables multiple simultaneous altimeter measurements at every time step and improves the filter's performance. Furthermore, if the vehicle is fitted with a DVL, velocity information will be available for more accurate propagation of the process model. With only a single-beam echo sounder, however, the filter may diverge due to multiple occurrences of similar terrain information within the bathymetry map [12].

In recent years, inter-vehicle acoustic communication has been used extensively for single beacon cooperative navigation [7], [13], [14], [15], [16], [17]. Although subject to extremely limited communication bandwidth and range, our previous work [14], [15] has demonstrated that it is indeed possible to minimize positioning error for a group of AUV's by maintaining one beacon vehicle that has good positioning information. In more recent work, the authors in [18] fused both acoustic ranging and bathymetric information (obtained by side-scan sonar) to better estimate a vehicle's position. Another related work was reported in [19], though the focus was on observability analysis using only the acoustic communications and depth measurements.

Despite advances in underwater communications, conventional methods of sharing a subset of particles [20] in the implementation of a distributed particle filter simply cannot be applied in the underwater domain due to extremely limited bandwidth and reliability. Various particle distribution aggregations have been developed as alternatives for alleviating communication limits [21], [22], but none of them have been applied in the underwater domain.

We adopt the filtering technique mentioned in [23] for the vehicle's position estimation. The main idea is that each vehicle runs (locally) a collaborative filter and broadcasts its local sufficient statistics (belief) at every communication period, instead of set of particles. We extend the measurement model to incorporate the information obtained from inter-vehicle acoustic communication, and this helps to alleviate the problem of over-confidence reported in [16], [17], since the individual vehicles' positions and error covariances are estimated solely from their own bathymetry measurements between the times of acoustic communication. The process model is driven using only the AUV's control inputs and a model that predicts AUV velocity based on the thruster control input and an onboard compass.

B. Vehicle's Process and Measurement Models

Let x, y be the easting and northing position of the vehicle, and c_x, c_y be the ocean current in the easting and northing direction, at the location of the vehicle. The discrete-time process model is described by:

$$\mathbf{x}_{t+1} = \mathbf{F}\mathbf{x}_t + \mathbf{G}_{u,t}\mathbf{u}_t + \zeta_{\mathbf{t}}. \tag{1}$$

where $\mathbf{x} = [x, y, c_x, c_y]^\top$ is the state vector, $\mathbf{F}$ and $\mathbf{G}_{u,t}$ are the state transition and input coupling matrices respectively. $\mathbf{u}_t$ is the input vector obtained from the thruster model and the onboard compass, while $\zeta_{\mathbf{t}}$ is the process noise vector, modeled as additive zero-mean Gaussian ($\zeta_t \sim \mathcal{N}(0, \sigma_\zeta^2)$), with covariance matrix, σ_ζ^2. The corresponding discrete-time measurement model is

$$\mathbf{y}_t = \mathbf{h}(\mathbf{x}_t) + \eta_{\mathbf{t}}. \tag{2}$$

where $\eta_{\mathbf{t}}$ is the measurement noise, modeled as an additive zero-mean Gaussian ($\eta_{\mathbf{t}} \sim \mathcal{N}(0, \sigma_\eta^2)$). $\mathbf{y}_t$ represents the vehicle's measurement at time t while $\mathbf{h}(\mathbf{x}_t)$ is the non-linear function that relates the bathymetric information at state $\mathbf{x}_t$ to the measurement.

C. Marginalized Particle Filter

Let N represent the number of particles used for the filter, and $\mathbf{x}_t^i$ represent the *i*th particle at time t. For the marginalized PF [23], the state vector is decomposed into two parts:

$$\mathbf{x} = \begin{bmatrix} \mathbf{x}^{\mathrm{pf}} \\ \mathbf{x}^{\mathrm{kf}} \end{bmatrix}. \tag{3}$$

where $\mathbf{x}^{\mathrm{pf}} = [x, y]^\top$ represents the position of the vehicle estimated by Particle Filter (PF) and $\mathbf{x}^{\mathrm{kf}} = [c_x, c_y]^\top$ represents the ocean current bias estimated by a Kalman Filter (KF). Similarly, the corresponding $\mathbf{F}$ and $\mathbf{G}_{u,t}$ matrices are decomposed into their corresponding PF and KF parts. The marginalized PF becomes:

Prediction:
The decomposed state vectors are propagated from time t to time $t+1$ with :

$$\mathbf{x}_{t+1}^{\mathrm{pf},i} = \mathbf{x}_t^{\mathrm{pf},i} + \mathbf{F}^{\mathrm{pf}}\mathbf{x}_t^{\mathrm{kf},i} + \mathbf{G}_u^{\mathrm{pf}}\mathbf{u}_t + \zeta_t^{\mathrm{pf}}. \tag{4}$$

$$\mathbf{x}_{t+1}^{\mathrm{kf},i} = \mathbf{F}^{\mathrm{kf}}\left[\hat{\mathbf{x}}_{t|t-1}^{\mathrm{kf},i} + \mathbf{K}_t\mathbf{V}_t\right]. \tag{5}$$

where $\mathbf{K}_t$ is the Kalman filter gain,
$\mathbf{V}_t = \mathbf{x}_{t+1}^{\mathrm{pf},i} - \mathbf{x}_t^{\mathrm{pf},i} - (\mathbf{F}^{\mathrm{pf}}\hat{\mathbf{x}}_{t|t-1}^{\mathrm{kf},i} + \mathbf{G}_u^{\mathrm{pf}}\mathbf{u}_t)$, and

$$\zeta_t^{\mathrm{pf}} = \mathcal{N}(0, \mathbf{F}^{\mathrm{pf}}\mathbf{P}_{t|t-1}^{\mathrm{kf}}(\mathbf{F}^{\mathrm{pf}})^\top + \mathbf{Q}^{\mathrm{pf}}). \tag{6}$$

with $\mathbf{Q}^{\mathrm{pf}}$ being the process noise intensity matrix.

Update:
The update step consists of updating the particle's relative weight (importance) based on its observation. Let w_t^i be the relative weight associated with ith particle at time t; it is updated according to [23] as:

$$w_t^i = w_{t-1}^i . p(\mathbf{y}_t \mid \mathbf{x}_t^i). \tag{7}$$

where $p(.)$ is the likelihood function of the observation $\mathbf{y}_t$ given the particles' predicted states $\mathbf{x}_t^i$ (w_0^i is initialized to $1/N$). With the updated weights, a point estimate of the current state $\hat{\mathbf{x}}_t$ can be estimated through:

$$\hat{\mathbf{x}}_t^{MMS} \simeq \sum_i^N w_t^i \mathbf{x}_t^i. \tag{8}$$

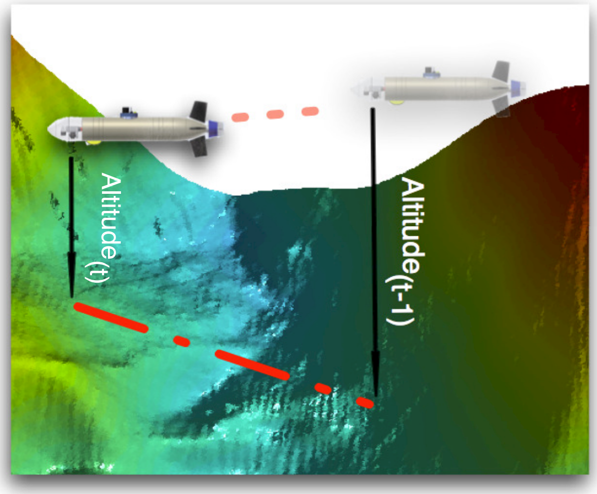

Fig. 2. Altitudes are measured and the difference in water depth (dashed-dot red line) are calculated from the measurements between the time-steps.

while the PF's covariance is approximated by:

$$P_t^{\text{pf}} = \sum_i^N w_t^i(\mathbf{x}_t^{\text{pf},i} - \hat{\mathbf{x}}_t^{\text{pf},MMS}) \cdot (\mathbf{x}_t^{\text{pf},i} - \hat{\mathbf{x}}_t^{\text{pf},MMS})^\top. \quad (9)$$

III. Measurement Model

The likelihood function in (7) depends on the vehicle's measurement model. For the case of single vehicle localization, the measurement consists of the water depth estimate (AUV altitude measurement + AUV depth measurement) at the location of the AUV. Whenever acoustic communication is available, the measurement model also incorporates information from other vehicles.

A. Single Vehicle

Without acoustic ranging and information from peer vehicles, the measurement only consists of the vehicle's water depth along its trajectory. Each of the particles keeps a history of the previous time step's measurement. It is then used to subtract the current time step's measurement to obtain the difference in water depth of the terrain between the two positions where the measurements were taken. Fig. 2 shows the altitude measurements as well as the difference in water depth deduced from the information between the time steps. Observing changes in water depth has the advantage of eliminating tidal offsets.

The weights of the particles are updated based on the likelihood function $p(.)$ of the measurement $\mathbf{y}_t$ given the predicted states $\mathbf{x}_t^i$. The measurement model takes into account the variation between the difference in water depth measured at the particles' predicted locations (with measurement noise from section II-B) and the true difference in water depth measured by the vehicle. The smaller the difference, the higher the weight that is assigned to the particular particle.

$$p(\mathbf{y}_t \mid \mathbf{x}_t^i) = p(\mathbf{y}_{t:t-1} - h(\mathbf{x}_{t:t-1}^{\text{pf},i})) \quad (10)$$

where the subscript $\mathbf{y}_{t:t-1}$ denotes the difference in water depth measured and $\mathbf{x}_{t:t-1}^i$ refers to the difference in position of particle i at time $t-1$ and at the current time t.

B. Multiple-vehicles with Acoustic Communication

Fitted with an acoustic modem, the vehicles are able to communicate and share information with other vehicles within their communication range. The vehicles in the team are assumed to have their system time synchronized. A simple round-robin scheduling is adopted such that each vehicle in the team, termed a Peer Vehicle (PV), broadcasts its local state information sequentially using acoustic communication. This information includes the vehicle's current position estimate, $\hat{\mathbf{x}}_t^{PV}$, its filter's estimated covariance matrix, P_t^{PV}, and the latest water depth measurement, $\mathbf{y}_t^{PV}$. When the acoustic signal is received by another vehicle, termed a Receiving Vehicle (RV), the time-of-arrival (TOA) can be calculated to determine the inter-vehicle distance, R. The measurement noise of R is not considered here, and is being addressed in our current work.

Since none of the vehicles in the team is equipped with high accuracy navigational sensors, the information received cannot be used directly to influence the measurement model presented in [24], as the PV may have accumulated significant error by the time the information is broadcast. Instead, the information from PV influences RV's particle distribution, and affects the corresponding weight computation in two separate stages:

1) Introduction of auxiliary particle set: A set of M auxiliary particles is added to the RV's original particle pool. These particles are randomly distributed within the boundary of the PV's error covariance, and the mean of the distribution is along a straight line between PV and RV at a distance R away from the PV, as illustrated in Fig. 3. The resultant $N+M$ particles then are weighted using the same likelihood function (10) as other particles. Intuitively, the introduction of the auxiliary particles modifies the distribution through the inter-vehicle constraints from ranging. The new distribution has the potential to alleviate divergence when the vehicle navigates over a flat terrain, until it enters another area that has more terrain variability.

2) Utilizing PV's water depth measurement: Given R, $\mathbf{y}_t^{PV}$ and P_t^{PV}, we assume that the probability of an RV particle representing the vehicle's true position is directly proportional to the probability of measuring $\mathbf{y}_t^{PV}$ within the ellipse described by the P_t^{PV}, and at a distance of R away from the particle's current position. For each of the $N+M$ particles p_i resulting from section III-B.1, a new set of particles, $\mathbf{p}^{int}$, is randomly generated along the arc formed by the intersection of a circle having radius R and centered at p_i, with P_t^{PV}. The average likelihood of $\mathbf{p}^{int}$ evaluated against $\mathbf{y}_t^{PV}$ contributes to the likelihood

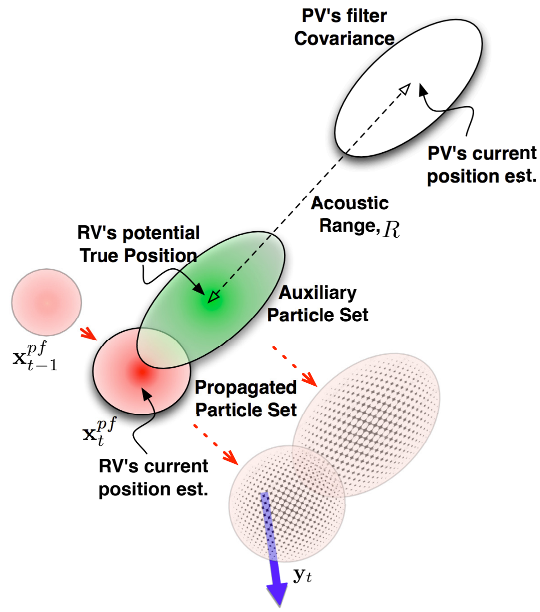

Fig. 3. Illustration shows the PV broadcast its current position estimate and error covariance via acoustic communication. Upon receiving it, the RV determines the distance (acoustic range) from the PV, and uses the PV's information to introduce new particle set (green ellipse) into its own particle set (red circle).

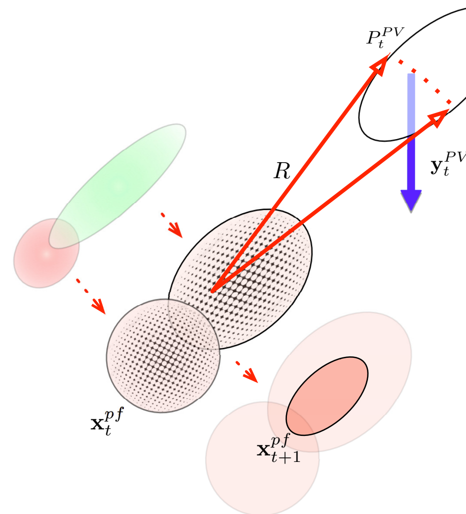

Fig. 4. Illustration shows information from PV is used by the RV's particles for the second stage likelihood evaluation. N particles are resampled with replacement from the pool of $N+M$ particles according to their relative normalized weights.

of p_i. This assumption makes use of PV's water depth measurement as well as the derived ranging information to further influence the local particles' distribution. This second stage likelihood evaluation is further illustrated in Fig. 4.

As a result, the particle's likelihood evaluation consists of an extra likelihood function whenever there is acoustic communication:

$$p(\mathbf{y}_t \mid \mathbf{x}_t^i) = p(\mathbf{y}_{t:t-1} - h(\mathbf{x}_{t:t-1}^{\mathrm{pf},i})) \times p(\mathbf{x}_t^{\mathrm{pf},i}, \hat{\mathbf{x}}_t^{PV}, P_t^{PV}, \mathbf{y}_t^{PV}, R) \quad (11)$$

Once all the particles undergo the likelihood evaluation, the original N particles are resampled with replacement, from the pool of $N+M$ particles, according to their relative normalized weights.

IV. Simulation Testing Setup and Results

Numerical experiments are conducted to assess the performance of these filters using bathymetric maps for two areas with distinct terrains. The first map is from waters near the St. John's Island, Singapore where depth varies from a few meters to around 30 meters, as shown in Fig. 5. The second map is from Charles River Basin, Boston (Fig. 8) where the terrain is flatter and patchy. We evaluate the localization performance using different numbers of vehicles, with and without acoustic communication, and under the influence of a simulated steady ocean current. The parameters shown in Table I are kept the same throughout all the runs, while the process and measurement noises are assumed Gaussian independent and drawn randomly at every propagation and measurement step. We present the localization performance in terms of the mean position error and current bias errors across all the vehicles.

TABLE I
Simulation Parameters

Parameter	Value
No. of particles	500
No. of auxiliary particles	300
Filter sampling time	1 s
Vehicles velocity	1.5 m/s
Sea current velocity	0.3 m/s
Ranging Period per vehicle	15 s
Ranging scheduling	Round-robin
Process noise std. dev., σ_ζ	$\begin{bmatrix} 0.1^2 & 0 & 0 & 0 \\ 0 & 0.1^2 & 0 & 0 \\ 0 & 0 & 0.1^3 & 0 \\ 0 & 0 & 0 & 0.1^3 \end{bmatrix}$ m
Measurement noise std. dev., σ_η	0.01 m

A. Simulation using St. John's Island bathymetry map

Fig. 5(a) shows the planned paths of five vehicles performing lawn-mowing surveying missions near the island. Assuming simple dead-reckoning, under the influence of a southward ocean current the resulting trajectories of the vehicles are shown in Fig. 5(b). From the simulated vehicle paths, depth measurements were drawn. Using the particle filter, these measurements were combined with control inputs for the planned paths, to generate estimated tracks. The objective of the filter is to minimize the error between the estimated tracks and the simulated paths, and to correctly estimate the ocean current model.

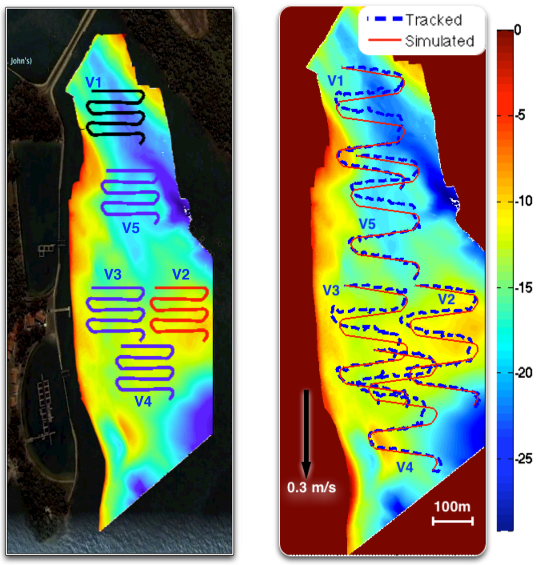

(a) (b)

Fig. 5. Planned paths and resultant trajectories of the vehicles performing surveying mission near St. John's island, Singapore. (a) Surveying paths of 5 vehicles (V1...V5) around St. John island, Singapore. (b) Vehicle trajectories (red lines) of the surveying paths due to the simulated sea current and the resultant trajectories tracked by the filter (dotted blue lines).

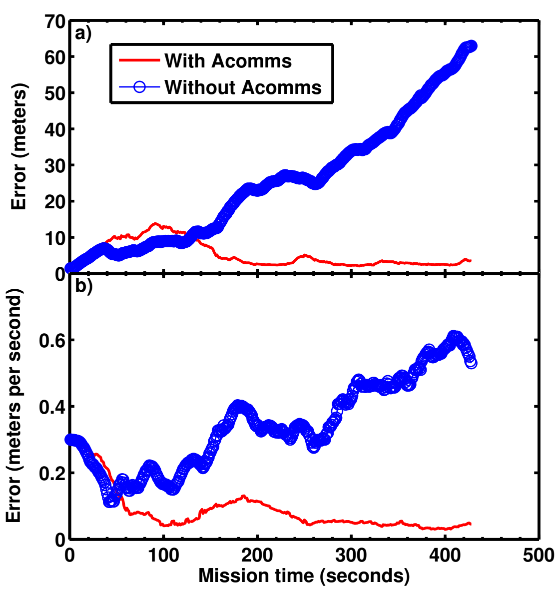

Fig. 6. The Average position and current velocity errors using St. John's Island bathymetry map. (a). Average position errors across five vehicles at the end of the simulated runs. Without acoustic communication, the position errors grow unbounded. (b). The average errors on the sea current speed estimation.

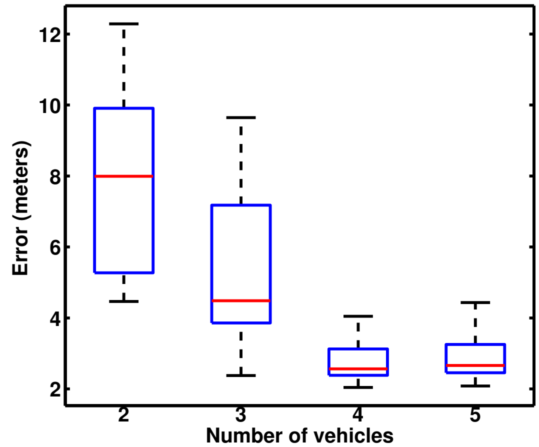

Fig. 7. Distribution of position estimation errors for different numbers of vehicles using St. John's Island bahtymetry map. Boxplots show the median and $25\% - 75\%$ quartiles while the whiskers are the smallest and greatest values.

In Fig. 6(a), we present position estimation errors averaged over all the vehicles in the team. Bathymetric-based localization is dramatically improved by acoustic communication; without information sharing between the vehicles, the filter fails to converge and position errors grow rapidly. The filters in each vehicle also reasonably track the ocean current model, as shown in Fig. 6(b). Since the vehicles are not equipped with any exteroceptive sensors, the accuracy of current estimation is important to the vehicle's navigational performance.

We varied the number of participating vehicles in the localization from two to five, while other parameters shown in Table I were held fixed. In Fig. 7 we see that the localization performance improves as the number of the vehicles in the team is increased, at least up to four. For a larger number of vehicles, the round-robin communication strategy lengthens the cycle time; longer update periods are a handicap to any filter.

The duration of an individual transmission's time slot is governed by propagation delay and other effects, so that generally one requires several seconds minimum [25]. We repeated the simulation runs with individual ranging intervals varying from 9 to 30 seconds; estimation errors increase slightly with time, but the trend is not significant.

B. *Hybrid experiment using autonomous surface vehicle in Charles River Basin*

The second set of tests was performed using a bathymetry map of the Charles River Basin, with altimeter measurements obtained from an autonomous surface vehicle (ASV). The ASV is fitted with a *Tritech*-PA500 single-beam altimeter, providing one-millimeter resolution when it operates in digital mode. Using the same parameters mentioned in Table I, a total of three lawn-mowing paths similar to those of Fig. 5(a) were planned. Under the influence of the simulated ocean

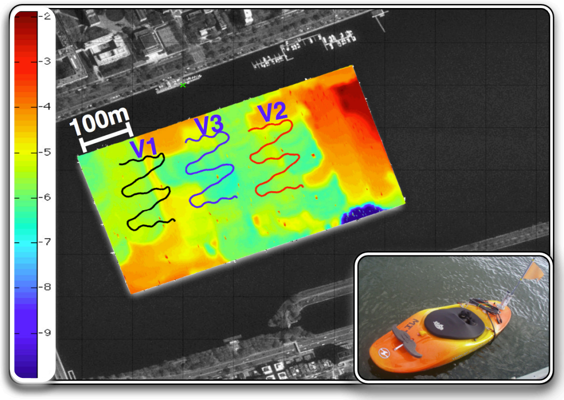

Fig. 8. Bathymetry map of Charles River and the simulated paths followed by our autonomous surface vehicle (insert) fitted with a single-beam altimeter.

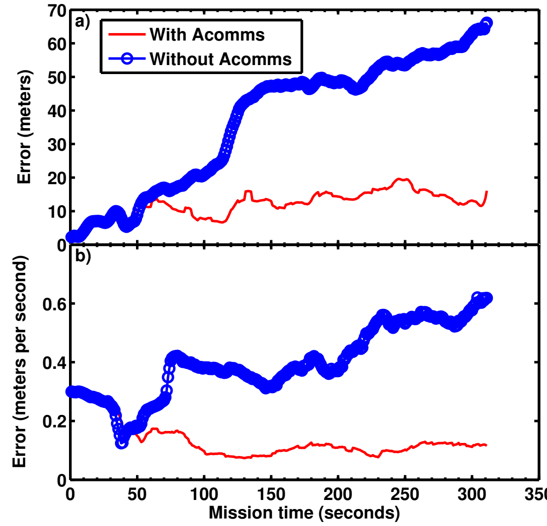

Fig. 9. Average position and velocity errors across three vehicles. (a).The average position estimation errors for all the vehicles using field data collected in Charles River, with a 25% acoustic communications drop rate. (b). The average current velocity errors for all the vehicles.

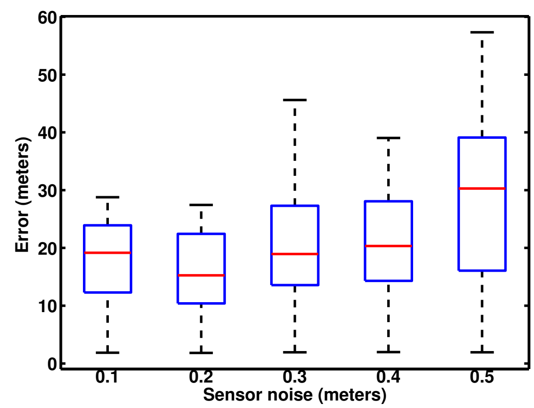

Fig. 10. Boxplot showing the distribution of position estimation errors in the Charles River case when the measurement noise of altimeter is increased.

current, we deformed the paths as for the St. John Island's case. The ASV was commanded to follow these three paths using high-precision RTK GPS as a ground truth, while collecting depth data. The resultant trajectories are shown in Fig. 8. The oscillating patterns on the trajectories were due to the surface waves and the ASV's onboard control system, which were not modeled in the filter.

Again, with the control input to the filter's process model derived from the planned paths, we carried out collaborative localization using the depth data as if it had been obtained by three separate vehicles. An acoustic communication packet broadcasting success rate of 75% [26] was simulated between the vehicles to emulate the acoustic channel's typical performance within this environment. Fig. 9 shows the average position and current bias errors accumulated by the vehicles. With only three vehicles in the team and a 25% packet loss rate, as well as the "unmodeled dynamic" caused by the vehicle's control system, the individual filters still managed to keep the errors around ten meters. As before, without acoustic communication, the filters failed to track the vehicles and to identify the current bias.

Errors in the second case (Fig. 9) are worse than in the first (Fig. 6). Besides the communication losses and control disturbances in the second case, there is a smaller number of vehicles, reducing the number of available constraints. A third factor is the quality of the map: St John's Island bathymetry was derived from high-resolution multi-beam sonar and INS, while the Charles River map was constructed by interpolating altimeter measurements that were collected separately by the ASV running a lawn-mowing pattern, with paths separated by five meters.

The assumption of 0.01 meters for the standard deviation of measurement noise may be too tight in some cases, especially for AUVs operating in deeper water. Fig. 10 shows the distribution of position estimation errors when the altimeter measurements are corrupted at higher noise levels. The collaborative filter is apparently robust up to 0.3 meters, with a graceful degradation of performance above that level. Other factors like the depth sensor's sampling frequency and terrain variability also affect the filter's localization performance, and will need to be considered in more detail. Overall, the simulation results presented so far confirm the crucial role of acoustic communication in aiding sensor-limited AUVs in performance collaborative localization.

V. Conclusion

In this paper, we have showed that it is feasible for a team of AUVs, each equipped with only a single-beam altimeter, a depth sensor, and an acoustic modem, to perform collaborative localization. In particular, we employed the Marginalized Particle Filter at each vehicle, and incorporated the information broadcast by other vehicles into each vehicle's local filter. We showed that the inter-vehicle communication is crucial for this capability, and that increasing the number of AUVs helps to improve the localization performance to a point. The resulting collaborative localization algorithm was also shown to be robust in handling higher levels of sensor noise and an unreliable communication channel.

VI. Acknowledgements

This work was supported by Singapore-MIT Alliance for Research and Technology (SMART) graduate fellowship. The authors wish to thank Hovergroup for obtaining the experimental data, Dr. Bharath Kaylan for his help in providing bathymetric maps and Ms. Ong Lee Lin for proofreading the manuscript.

References

[1] A. Matos, N. Cruz, A. Martins, and F. Lobo Pereira, "Development and implementation of a low-cost LBL navigation system for an AUV," in *OCEANS '99 MTS/IEEE. Riding the Crest into the 21st Century*, vol. 2, 1999, pp. 774 –779.

[2] P. Rigby, O. Pizarro, and S. Williams, "Towards geo-referenced AUV navigation through fusion of USBL and DVL measurements," in *OCEANS '06*, 2006, pp. 1 –6.

[3] A. Alcocer, P. Oliveira, and A. Pascoal, "Study and implementation of an EKF GIB-based underwater positioning system," *Control Engineering Practice*, vol. 15, no. 6, pp. 689 – 701, 2007.

[4] D. Meduna, S. Rock, and R. McEwen, "Closed-loop terrain relative navigation for AUVs with non-inertial grade navigation sensors," in *Autonomous Underwater Vehicles (AUV), 2010 IEEE/OES*, 2010, pp. 1–8.

[5] S. Carreno, P. Wilson, P. Ridao, and Y. Petillot, "A survey on terrain based navigation for AUVs," in *OCEANS '10*, 2010, pp. 1–7.

[6] B. Kalyan and M. Chitre, "A feasibility analysis on using bathymetry for navigation of autonomous underwater vehicles," in *Proceedings of the 28th Annual ACM Symposium on Applied Computing*, ser. SAC '13. New York, NY, USA: ACM, 2013, pp. 229–231.

[7] S. E. Webster, R. M. Eustice, H. Singh, and L. L. Whitcomb, "Advances in single-beacon one-way-travel-time acoustic navigation for underwater vehicles," *The International Journal of Robotics Research*, vol. 31, no. 8, pp. 935–950, 2012.

[8] A. Doucet, S. Godsill, and C. Andrieu, "On sequential monte carlo sampling methods for bayesian filtering," *Statistics and Computing*, vol. 10, no. 3, pp. 197–208, July 2000.

[9] T. Schon, F. Gustafsson, and P.-J. Nordlund, "Marginalized particle filters for mixed linear/nonlinear state-space models," *Signal Processing, IEEE Transactions on*, vol. 53, no. 7, pp. 2279–2289, 2005.

[10] F. Teixeira, A. Pascoal, and P. Maurya, "A novel particle filter formulation with application to terrain-aided navigation," in *Proc. IFAC Workshop on Navigation, Guidance and Control of Underwater Vehicles (NGCUV'2012), Porto, Portugal*, 2012, pp. 10–12.

[11] N. Fairfield and D. Wettergreen, "Active localization on the ocean floor with multibeam sonar," in *OCEANS '08*, 2008, pp. 1–10.

[12] I. Nygren and M. Jansson, "Terrain navigation for underwater vehicles using the correlator method," *Oceanic Engineering, IEEE Journal of*, vol. 29, no. 3, pp. 906–915, 2004.

[13] M. F. Fallon, G. Papadopoulos, J. J. Leonard, and N. M. Patrikalakis, "Cooperative auv navigation using a single maneuvering surface craft," *The International Journal of Robotics Research*, vol. 29, no. 12, pp. 1461–1474, 2010.

[14] M. Chitre, "Path planning for cooperative underwater range-only navigation using a single beacon," in *Autonomous and Intelligent Systems (AIS), 2010 International Conference on*, 2010, pp. 1 –6.

[15] Y. T. Tan and M. Chitre, "Single beacon cooperative path planning using cross-entropy method," in *IEEE/MTS OCEANS, Kona, Hawaii*, September 2011.

[16] A. Bahr, M. Walter, and J. Leonard, "Consistent cooperative localization," in *IEEE International Conference on Robotics and Automation (ICRA), Kobe, Japan*, May 2009.

[17] S. Webster, J. Walls, L. Whitcomb, and R. Eustice, "Decentralized extended information filter for single-beacon cooperative acoustic navigation: Theory and experiments," *Robotics, IEEE Transactions on*, vol. 29, no. 4, pp. 957–974, 2013.

[18] M. F. Fallon, M. Kaess, H. Johannsson, and J. J. Leonard, "Efficient AUV navigation fusing acoustic ranging and side-scan sonar," in *IEEE International Conference on Robotics and Automation (ICRA),Shanghai, China*, May 2011.

[19] G. Antonelli, F. Arrichiello, S. Chiaverini, and G. Sukhatme, "Observability analysis of relative localization for auvs based on ranging and depth measurements," in *IEEE International Conference on Robotics and Automation (ICRA), Anchorage, Alaska*, May 2010.

[20] M. Rosencrantz, G. Gordon, and S. Thrun, "Decentralized sensor fusion with distributed particle filters," in *Proceedings of the Nineteenth conference on Uncertainty in Artificial Intelligence*, ser. UAI'03. San Francisco, CA, USA: Morgan Kaufmann Publishers Inc., 2003, pp. 493–500.

[21] B. Jiang and B. Ravindran, "Completely distributed particle filters for target tracking in sensor networks," in *Parallel Distributed Processing Symposium (IPDPS), 2011 IEEE International*, 2011, pp. 334–344.

[22] X. Sheng, Y.-H. Hu, and P. Ramanathan, "Distributed particle filter with GMM approximation for multiple targets localization and tracking in wireless sensor network," in *Information Processing in Sensor Networks, 2005. IPSN 2005. Fourth International Symposium on*, 2005, pp. 181–188.

[23] F. Teixeira, "Terrain-aided navigation and geophysical navigation of autonomous underwater vehicles," Ph.D. dissertation, Dynamical Systems and Ocean Robotics Lab, Lisbon, 2007.

[24] P. Maurya, F. C. Teixeira, and A. Pascoal, "Complementary terrain/single beacon-based AUV navigation," in *Proc IFAC Workshop on Navigation, Guidance and Control of Underwater Vehicles (NGCUV'2012), Porto, Portugal*, 2012, pp. 10–12.

[25] J. Heidemann, M. Stojanovic, and M. Zorzi, "Underwater sensor networks: applications, advances and challenges," *Philosophical Transactions of the Royal Society A: Mathematical, Physical and Engineering Sciences*, vol. 370, no. 1958, pp. 158–175, 2012.

[26] M. Cheung, J. Leighton, and F. Hover, "Multi-armed bandit formulation for autonomous mobile acoustic relay adaptive positioning," in *Proc. IEEE International Conference on Robotics and Automation (ICRA)*, 2013.